J. Fluid Mech. (1971), *vol.* 46, *part* 3, *pp.* 417–445
Printed in Great Britain

Calculation of three-dimensional turbulent boundary layers

By P. BRADSHAW
National Physical Laboratory, Teddington†

(Received 2 June 1970)

The two-dimensional prediction method of Bradshaw, Ferriss & Atwell (1967), which was based on the empirical conversion of the turbulent energy equation into a 'transport' equation for shear stress, is extended to three-dimensional flows satisfying the boundary-layer approximation (which excludes flows near bluff obstacles or streamwise corners). Predictions, using exactly the same empirical data as in two-dimensional flow, agree to within the likely experimental error with a variety of experiments on 'infinite' swept wings.

1. Introduction

In a three-dimensional laminar boundary layer, the shear stress is equal in magnitude and direction to μ times the velocity gradient, whose components in the x and z directions are $\partial U/\partial y$ and $\partial W/\partial y$, where y is the direction normal to the surface. In a turbulent flow the Reynolds shear stress, whose components in the x and z directions are $-\rho\overline{uv}$ and $-\rho\overline{vw}$, is not simply related to the velocity gradient either in magnitude or direction: the reasons are discussed in § 2.

However, existing prediction methods for three-dimensional turbulent boundary layers nearly all assume, explicitly or implicitly, that the shear stress, or the shear stress profile at given x, z, is uniquely related to the velocity gradient or the velocity profile. One of the few straightforward and explicit examples is the entrainment method of Cumpsty & Head (1967*a*, *b*) in which the dimensionless entrainment rate is assumed to be the same function of the streamwise velocity-profile shape as in two dimensions. The method of Nash (1969) is a hybrid: the shear stress is assumed to have the same direction as the velocity gradient ('isotropic eddy viscosity') but its magnitude is predicted from an empirical 'transport' equation (an equation for the rate of change of shear stress along a mean streamline) similar to that derived for two-dimensional flow by Bradshaw *et al.* (1967). Since the difference between the directions of the velocity-gradient and shear-stress vectors seems to be more noticeable in practice than the difference in their relative magnitude, it is advisable to derive 'transport' equations for both the magnitude *and* direction of the shear stress or, equivalently, for both the components $-\rho\overline{uv}$ and $-\rho\overline{vw}$.

The empirical transport equation of Bradshaw *et al.* was derived from the (exact) turbulent energy equation, which is better documented experimentally than the (exact) transport equation for $-\overline{uv}$ (equation (1), below). However, the

† Present address: Department of Aeronautics, Imperial College, London S.W. 7

empirical equation, once derived, can equally well be regarded as an empirical approximation to the exact equation for $-\overline{uv}$: to extend the prediction method to three-dimensional flow we can simply make the analogous approximation to the exact $-\overline{vw}$ equation (equation (2), below) and this is done in the present paper. The three empirical functions used in the prediction method nominally become functions of the shear stress vector, but only one of the three is likely to depend appreciably on the direction of the shear stress. The present predictions for three-dimensional flow in a variety of pressure gradients use the same empirical data as the two-dimensional method, data taken solely from two-dimensional flow and almost exclusively from constant-pressure flow. The essential justification for this is the plausible hypothesis that moderate three-dimensionality of the mean flow should not materially affect the scalar properties of the turbulence because turbulence is *always* three-dimensional: the practical justification is that the agreement with experiment is generally good.

'Moderate three-dimensionality' does not imply a restriction to small cross-flow (i.e. a small angle between the streamlines in the free stream and at the surface): it implies only that the change in direction of the velocity gradient over a vertical distance equal to a typical eddy wavelength shall be small, and this restriction should be satisfied by most swept-wing boundary layers. The only flows specifically excluded, from this as from all other 'boundary-layer' methods, are those for which the boundary-layer approximation is not satisfied. In three-dimensional flow the boundary-layer approximation requires that velocity gradients normal to the surface shall be much larger than velocity gradients parallel to the surface, and that the radii of curvature of the surface shall be much larger than the boundary-layer thickness. Unfortunately this excludes flows of practical interest, near wing tips, wing-body junctions and other nearly streamwise corners or separation lines, as well as blunt three-dimensional obstacles in initially two-dimensional boundary layers. Corner flows, like flows in non-circular ducts, are driven by normal-stress gradients as well as shear-stress gradients, so that additional Reynolds stress transport equations are needed: we have no immediate hope of an extension of the method to these flows, although Donaldson, Sullivan & Rosenbaum (1970) have proposed transport equations for the three normal stresses (and the shear stress) in two-dimensional flow. In flows round bluff obstacles, stress gradients of any kind are small compared with pressure gradients, so that Bernoulli's equation applies, except very near the surface where local-equilibrium assumptions such as the mixing-length formula can, as usual, be used to predict the shear stress: it follows that assumptions for the Reynolds stresses in the outer layer cannot usefully be checked by comparison of *mean-flow* predictions with experiments on bluff obstacles, although direct Reynolds stress measurements in such flows would afford a very searching test of turbulence models (see § 8.3).

In § 2 of this paper we derive two differential equations for the two components of shear stress by logical extensions of the arguments used in two-dimensional flow. In § 3 the boundary conditions are discussed, and in § 5 we outline the method of solution used in the calculations presented in § 8. Sections 4, and 6 and 7 deal with special cases and specific difficulties.

2. Shear stress transport equations

Some of the material in this section first appeared in a short paper in Kline *et al.* (1969): a similar analysis has been given semi-independently by Wesseling (1969).

The following equations for the components of the turbulent shear-stress vector $\boldsymbol{\tau} \equiv -\rho\overline{uv},\ -\rho\overline{vw}$ in the xy, yz planes, where x, y and z are rectangular Cartesian co-ordinates, *not* streamline co-ordinates, can be derived from the incompressible Navier–Stokes equations; like the Navier–Stokes equations they give only the *rate of change* of the desired quantity along a mean streamline or equivalently the rate at which the quantity is being transported out of a unit control volume—hence the name 'transport equations':

$$\left(U\frac{\partial}{\partial x}+V\frac{\partial}{\partial y}+W\frac{\partial}{\partial z}\right)(-\overline{uv})=\frac{D}{Dt}(-\overline{uv})=\overline{v^2}\frac{\partial U}{\partial y}-\overline{\frac{p'}{\rho}\left(\frac{\partial u}{\partial y}+\frac{\partial v}{\partial x}\right)}$$
$$+\frac{\partial}{\partial y}\left(\overline{\frac{p'u}{\rho}}+\overline{uv^2}\right)-\nu(\overline{u\nabla^2 v}+\overline{v\nabla^2 u}), \quad (1)$$

$$\frac{D}{Dt}(-\overline{vw})=\overline{v^2}\frac{\partial W}{\partial y}-\overline{\frac{p'}{\rho}\left(\frac{\partial v}{\partial z}+\frac{\partial w}{\partial y}\right)}+\frac{\partial}{\partial y}\left(\overline{\frac{p'w}{\rho}}+\overline{v^2 w}\right)-\nu(\overline{v\nabla^2 w}+\overline{w\nabla^2 v}). \quad (2)$$

The equations are exact except that the boundary-layer approximation has been used. They show that if the velocity gradient changes, only $D\tau/Dt$, and not τ, changes at once (Townsend 1956).

Since the viscous-dependent part of the turbulence is isotropic except in and near the viscous sublayer, the viscous terms in (1) and (2) are negligible elsewhere (the terms like $\nu\overline{u\nabla^2 u}$ in the analogous equations for the normal stresses represent dissipation). The first term on the right of each equation represents generation of shear stress by the mean velocity gradient, and the third represents 'diffusion' or turbulent transport of shear stress normal to the surface. The second term, the mean product of the fluctuating pressure p' and the fluctuating rate of strain (hereafter called the 'pressure-strain term' for brevity) represents the 'isotropizing'† effect of pressure fluctuations: similar terms exchange energy between the normal-stress components, but shear stress is not an energy quantity and is not conserved in the strict sense of the word, so that the shear stress that is destroyed by the pressure-strain term does not *go* anywhere. Since we cannot at present measure pressure fluctuations within the flow with any assurance of accuracy, we know very little about the pressure-strain term. As the generation term is straightforward and the diffusion term usually small enough for crude approximations to suffice, the problem of deriving tractable shear-stress equations from equations (1) and (2) reduces to the problem of finding out how the pressure-strain term behaves.

Now, the shear stress transport equation used in the two-dimensional method of Bradshaw *et al.* can be regarded as an empirical modification of (1). It is

$$\frac{D(-\overline{uv})}{Dt}=2a_1\left(-\overline{uv}\frac{\partial U}{\partial y}-\text{energy dissipation}-\text{energy diffusion}\right), \quad (3)$$

† An unlovely word, formed by analogy with 'homogenize': suggestions for a more euphonious alternative are invited.

where a_1 is defined as $-\overline{uv}/(\overline{u^2}+\overline{v^2}+\overline{w^2})$ and is taken to be a constant, 0·15 (for a discussion, see Bradshaw 1967). The left-hand sides of (1) and (3) are identical and we may expect that, if the derivation of (3) is close to the truth, the 'diffusion' term in (1) will be equal to the 'diffusion' term in (3), because they represent the same process of turbulent transport in the y direction. Subtracting (3) from (1), neglecting the viscous terms in the latter, gives

$$\overline{\frac{p'}{\rho}\left(\frac{\partial u}{\partial y}+\frac{\partial v}{\partial x}\right)} = (\overline{v^2}+2a_1\overline{uv})\frac{\partial U}{\partial y}+2a_1.(\text{energy dissipation}), \tag{4}$$

so this is what the assumptions of Bradshaw *et al.*, leading to (3), imply for the pressure-strain term in (1). It is the sum of a 'negative production', directly opposing the generation of shear stress by the term $\overline{v^2}\partial U/\partial y$ in (1), and of a direct destruction of shear stress, analogous to energy dissipation. This dual behaviour of the pressure-strain term is plausible when one notes that the Poisson equation for the fluctuating pressure in a two-dimensional boundary layer is

$$\frac{\nabla^2 p'}{\rho} = 2\frac{\partial U}{\partial y}.\frac{\partial v}{\partial x}+\frac{\partial^2(u_iu_j-\overline{u_iu_j})}{\partial x_i\partial x_j} \tag{5}$$

(the second term being summed over all components and all directions) which has obvious similarities with (4). Equation (5) has to be integrated over all space to get p' but the part of p' that correlates with the rate of strain at a given point will presumably be the part generated near that point so that the local value of $\partial U/\partial y$ will appear in the pressure-strain term. Crow (1968) has calculated the part of the pressure-strain term that depends on $\partial U/\partial y$, for the special case of a homogeneous mean shear suddenly applied to initially isotropic turbulence. Defining a_3 as $(\overline{v^2}+2a_1\overline{uv})/\overline{v^2}$, and a length L as $(-\overline{uv})^{\frac{3}{2}}/(\text{energy dissipation})$, (4) becomes

$$\overline{\frac{p'}{\rho}\left(\frac{\partial u}{\partial y}+\frac{\partial v}{\partial x}\right)} = a_3\overline{v^2}\frac{\partial U}{\partial y}+2a_1.\frac{(-\overline{uv})^{\frac{3}{2}}}{L}. \tag{6}$$

We expect a_3 to be nearly constant for the same reasons as a_1.

In a three-dimensional flow, the simplest and most obvious assumption to make about the pressure-strain term, now a vector with components

$$\overline{(p'/\rho)(\partial u/\partial y+\partial v/\partial x)}, \quad \overline{(p'/\rho)(\partial v/\partial z+\partial w/\partial y)},$$

is that it is again the sum of a direct destruction of shear stress (a vector having the same direction as the shear stress $\boldsymbol{\tau}$ which now has components $-\rho\overline{uv}$, $-\rho\overline{vw}$) and of a 'negative production' (a vector having the same direction as the velocity gradient $\partial\mathbf{U}/\partial y$ which now has components $\partial U/\partial y$, $\partial W/\partial y$). Following the general hypothesis that scalar properties of the turbulence are unaltered by moderate three-dimensionality, we assume that a_1, a_3 and L will have the same values as in two dimensions if defined as $|\boldsymbol{\tau}|/\rho(\overline{u^2}+\overline{v^2}+\overline{w^2})$, $(\overline{v^2}-2a_1|\boldsymbol{\tau}|/\rho)/\overline{v^2}$ and $(|\boldsymbol{\tau}|/\rho)^{\frac{3}{2}}/$(energy dissipation)—essentially we assume that $(|\boldsymbol{\tau}|/\rho)^{\frac{1}{2}}$ is a typical velocity scale for the turbulence. Then the *vector* pressure-strain term becomes

$$a_3\overline{v^2}\frac{\partial\mathbf{U}}{\partial y}+\frac{2a_1}{L}\left|\frac{\boldsymbol{\tau}}{\rho}\right|^{\frac{1}{2}}\frac{\boldsymbol{\tau}}{\rho},$$

the second term in this expression being a vector of magnitude $2a_1(|\boldsymbol{\tau}|/\rho)^{\frac{3}{2}}/L$ having the same direction as $\boldsymbol{\tau}$. Writing τ_x for $-\rho\overline{uv}$ and τ_z for $-\rho\overline{vw}$, the pressure-strain terms in (1) and (2) become

$$a_3\overline{v^2}\frac{\partial U}{\partial y}+\frac{2a_1}{L}\left|\frac{\boldsymbol{\tau}}{\rho}\right|^{\frac{1}{2}}\tau_x$$

and

$$a_3\overline{v^2}\frac{\partial W}{\partial y}+\frac{2a_1}{L}\left|\frac{\boldsymbol{\tau}}{\rho}\right|^{\frac{1}{2}}\tau_z.$$

Substituting in (1) and (2) we obtain

$$\frac{D\tau_x}{Dt}=2a_1\left(|\boldsymbol{\tau}|\frac{\partial U}{\partial y}-\frac{|\boldsymbol{\tau}/\rho|^{\frac{1}{2}}\tau_x}{L}\right)-(\tau_x\,\text{diffusion}),\tag{7}$$

$$\frac{D\tau_z}{Dt}=2a_1\left(|\boldsymbol{\tau}|\frac{\partial W}{\partial y}-\frac{|\boldsymbol{\tau}/\rho|^{\frac{1}{2}}\tau_z}{L}\right)-(\tau_z\,\text{diffusion}).\tag{8}$$

Note that $a_1=|\boldsymbol{\tau}|/\rho(\overline{u^2}+\overline{v^2}+\overline{w^2})$ and that a_3 does not appear as such. These equations naturally reduce, in two-dimensional flow, to equation (3).†

The magnitude of the 'diffusion' vector in (7) and (8) should be nearly the same as in two dimensions but its direction will depend on some functional of the shear-stress direction throughout the boundary layer (although it is unlikely that large changes in shear stress direction—or magnitude—near the surface will have much effect on the outer layer). This is the only extra piece of experimental information that we need to extend the calculation method of Bradshaw *et al.* to three dimensions (though confirmation of the above analysis is obviously desirable). In the calculations presented here we have simply assumed that the quantity whose gradient is the diffusion vector has the same direction as the local shear stress and written it as $2a_1G|\boldsymbol{\tau}_{\max}/\rho|^{\frac{1}{2}}\boldsymbol{\tau}/\rho$ where G is approximated by $|\boldsymbol{\tau}_{\max}/\rho U_1^2|^{0\cdot5}$ times a scalar function of y/δ, as in two-dimensional flow. This assumption is plausible physically, convenient numerically, and almost certainly accurate enough for wing-type boundary layers because the main influence of G is that it determines the rate of entrainment of fluid at the edge of the boundary layer: entrainment is a scalar so that only the magnitude of G is really important. The final equations for the rate of change of the shear stress components along a mean streamline now become

$$\frac{1}{2a_1\rho}\frac{D\tau_x}{Dt}=\frac{|\boldsymbol{\tau}|}{\rho}\frac{\partial U}{\partial y}-\frac{(|\boldsymbol{\tau}|/\rho)^{\frac{1}{2}}.\tau_x/\rho}{L}-\frac{\partial}{\partial y}(G(|\boldsymbol{\tau}_{\max}|/\rho)^{\frac{1}{2}}\tau_x/\rho)\tag{9}$$

† Before devising the present argument we derived equations similar to (7) and (8) solely from the three-dimensional form of the turbulent energy equation. The argument for the 'dissipation' terms (those containing L) was that energy dissipation would reduce the magnitude of τ without altering its direction: the result is the same as in equations (7) and (8). The production term in the turbulent energy equation is $\boldsymbol{\tau}.\partial\mathbf{U}/\partial y$, a scalar, and it was argued that the shear stress associated with this newly-produced energy should be in the direction of the velocity gradient: the resulting 'production' term is $(\cos\theta)$ times the 'production' term in (7) and (8), where θ is the angle between $\boldsymbol{\tau}$ and $\partial\mathbf{U}/\partial y$. Usually θ will be small: it is assumed zero in the mixing length or eddy viscosity approaches. Therefore we can equate its cosine to unity and reconcile the two derivations of (7) and (8).

and
$$\frac{1}{2a_1\rho}\frac{D\tau_z}{Dt} = \frac{|\boldsymbol{\tau}|}{\rho}\frac{\partial W}{\partial y} - \frac{(|\boldsymbol{\tau}|/\rho)^{\frac{1}{2}}.\tau_z/\rho}{L} - \frac{\partial}{\partial y}(G(|\boldsymbol{\tau}_{\max}|/\rho)^{\frac{1}{2}}\tau_z/\rho). \tag{10}$$

In the more general case G would be replaced by G_x in (9) and G_z in (10).

If we rewrite (9) and (10) to give us the rates of change of the magnitude and direction of the shear stress, we get

$$\frac{1}{2a_1\rho}\frac{D|\boldsymbol{\tau}|}{Dt} = \left(\frac{\tau_x}{\rho}\frac{\partial U}{\partial y} + \frac{\tau_z}{\rho}\frac{\partial W}{\partial y}\right) - \frac{(|\boldsymbol{\tau}|/\rho)^{\frac{3}{2}}}{L} - \frac{\partial}{\partial y}\left(G\frac{|\boldsymbol{\tau}|}{\rho}\left(\frac{|\boldsymbol{\tau}|_{\max}}{\rho}\right)^{\frac{1}{2}}\right) \tag{11}$$

and
$$\frac{1}{2a_1}\frac{D(\tau_z/\tau_x)}{Dt} = \frac{|\boldsymbol{\tau}|}{\tau_x^2}\left(\tau_x\frac{\partial W}{\partial y} - \tau_z\frac{\partial U}{\partial y}\right) - G\left(\frac{\boldsymbol{\tau}_{\max}}{\rho}\right)^{\frac{1}{2}}\frac{\partial}{\partial y}\left(\frac{\tau_z}{\tau_x}\right). \tag{12}$$

The first equation is exactly the scalar form of the turbulent energy equation with the same definitions of a_1, L and G as in two dimensions: the second equation shows that even with a scalar function for G a change in shear stress direction with y will produce a change of shear stress direction with distance along a streamline. The 'dissipation' term containing L does not affect the shear stress direction, whereas the rate of change of shear stress direction caused by the 'production' term is proportional to the sine of the angle between the shear stress vector and the velocity gradient vector.

Equations (9) and (10) are to be solved with the momentum equations

$$\frac{DU}{Dt} = -\frac{1}{\rho}\frac{\partial p}{\partial x} + \frac{1}{\rho}\frac{\partial \tau_x}{\partial y}, \tag{13}$$

$$\frac{DW}{Dt} = -\frac{1}{\rho}\frac{\partial p}{\partial z} + \frac{1}{\rho}\frac{\partial \tau_z}{\partial y}, \tag{14}$$

and the continuity equation
$$\frac{\partial U}{\partial x} + \frac{\partial V}{\partial y} + \frac{\partial W}{\partial z} = 0. \tag{15}$$

In compressible flow, a few extra terms appear, but the character of the equations is the same.

As in two-dimensional flow we expect that, near the surface but outside the viscous sublayer, the rate of change of shear stress along a streamline, and the diffusion terms, will become small compared with the other two terms: in this case equations (9) and (10) reduce to

$$\frac{|\boldsymbol{\tau}|}{\rho}\frac{\partial U}{\partial y} = \left|\frac{\boldsymbol{\tau}}{\rho}\right|^{\frac{1}{2}}\frac{\tau_x/\rho}{L},$$
$$\frac{|\boldsymbol{\tau}|}{\rho}\frac{\partial W}{\partial y} = \left|\frac{\boldsymbol{\tau}}{\rho}\right|^{\frac{1}{2}}\frac{\tau_z/\rho}{L},$$

so that near the surface the direction of the shear stress is the same as the direction of the mean velocity gradient and its magnitude is

$$|\boldsymbol{\tau}| = (\tau_x^2+\tau_z^2)^{\frac{1}{2}} = \rho L^2((\partial U/\partial y)^2+(\partial W/\partial y)^2) = \rho L^2|\partial \mathbf{U}/\partial y|^2.$$

Therefore, as in two dimensions, the shear stress equations reduce to the 'mixing length' formula near the surface. In the outer part of the flow the directions of the velocity and shear stress do not in general coincide and the present method is virtually certain to be an improvement on the 'mixing length' or 'eddy viscosity' assumption that the directions coincide everywhere.

3. Boundary conditions

The components of the external stream velocity, U_1 and W_1, are assumed given: it has been pointed out by Kovasznay & Hall (1967) that since the external stream is supposed to be irrotational $\partial U_1/\partial z - \partial W_1/\partial x$ must be zero so that U_1 and W_1 cannot be chosen independently. The outer boundary condition, at $y = \delta$, is $U \to U_1$, $W \to W_1$, $\tau_x, \tau_z \to 0$: the limiting direction of the shear stress, τ_z/τ_x, is not, and does not have to be, prescribed. Near the surface it is convenient to match the calculations to the velocity profile given by the mixing length formula: as in two dimensions, it is necessary to estimate the shear stress gradient(s) between the surface and the matching point and, as in two dimensions, the shear stress gradient will not be equal to the pressure gradient because of the acceleration terms, which we must therefore estimate. The assumption we have made for this latter purpose in two dimensions, that the velocity profile follows a one-fifth power law between the surface and the matching point, should suffice for both the velocity components in three dimensions. It is not accurate for the component normal to the wall shear stress vector, but, at least in the case of an infinite swept wing, where $\partial p/\partial z = 0$, this is important only near separation ($\tau_w \to \tau_z$, $\tau_x \to 0$) and there the U component acceleration terms are small near the surface since the U component itself is small. Therefore the numerical accuracy for the infinite swept wing should be, and is, nearly as good as in two dimensions except very close to separation.

We have assumed that τ_x, τ_z *and* τ vary linearly between values at the wall, $y = 0$, and at the matching point, $y = y(1)$: since $|\boldsymbol{\tau}| = (\tau_x^2 + \tau_z^2)^{\frac{1}{2}}$ the three assumptions are not exactly compatible but the error involved should be no larger than the error already incurred by assuming linear variations of τ_x and τ_z. We write $\tau_x = \tau_{xw} + \alpha_x y$, $\tau_z = \tau_{zw} + \alpha_z y$ and $\boldsymbol{\tau} = \boldsymbol{\tau}_w + \boldsymbol{\alpha} y$, where α, the magnitude of $\boldsymbol{\alpha}$, is taken as $((\tau_x^2(1) + \tau_z^2(1))^{\frac{1}{2}} - \tau_w)/y(1)$ (which gives the best accuracy when *either* α_x *or* α_z is large, the cases when these stress gradients are most likely to be important). The mixing length formulae then become

$$\frac{\partial U}{\partial y} = \frac{\tau_x/\rho}{(|\boldsymbol{\tau}|/\rho)^{\frac{1}{2}} Ky} \doteq \frac{\tau_{xw} + \alpha_x y}{\rho^{\frac{1}{2}}(\tau_w + \alpha y)^{\frac{1}{2}} Ky},$$

$$\frac{\partial W}{\partial y} = \frac{\tau_{zw} + \alpha_z y}{\rho^{\frac{1}{2}}(\tau_w + \alpha y)^{\frac{1}{2}} Ky}.$$

Integrating, and requiring compatibility with the logarithmic law for small α_x, α_z and α, we obtain

$$U = \frac{\tau_{xw}}{\rho^{\frac{1}{2}}\tau_w^{\frac{1}{2}}} \frac{1}{K}\left[\log \frac{(\tau_w/\rho)^{\frac{1}{2}} y}{\nu} + A + 2\log \frac{2}{1 + (1 + (\alpha y/\tau_w))^{\frac{1}{2}}}\right] + \frac{2\alpha_x}{K\alpha}\left(\frac{\tau_w}{\rho}\right)^{\frac{1}{2}} [(1 + (\alpha y/\tau_w))^{\frac{1}{2}} - 1] \quad (16)$$

where the last term can be written

$$2\frac{\alpha_x y}{K\rho^{\frac{1}{2}}\tau_w^{\frac{1}{2}}} \frac{1}{(1 + (\alpha y/\tau_w))^{\frac{1}{2}} + 1},$$

and a similar expression for W. Strictly the additive constant of integration A, representing the velocity change across the viscous sublayer, should be a vector

function of the dimensionless shear stress gradient near the surface, $\alpha\nu\rho^{\frac{1}{2}}/\tau_w^{\frac{3}{2}}$. In two-dimensional flow the variation of A with shear stress gradient seems to be negligible, except near separation where A is in any case small compared to the other terms in the two-dimensional version of (16). Mainly owing to uncertainty in surface shear stress measurement, existing data on the inner layer in three-dimensional flow are insufficient to document the variation of A, but there is no reason to expect the variation to be larger than in two-dimensional flow for a given shear stress gradient. Again, there is no reason to expect the shear stress gradient near the surface to be larger than in two-dimensional flow: it can scarcely be larger than the pressure gradient and the only case in which pressure gradients are larger in three-dimensional flow than in two dimensions is when the radius of curvature of the external streamlines in plan view is not very large compared to the boundary-layer thickness—which implies violation of the boundary-layer approximation anyway. Therefore we have taken $A = 2{\cdot}0$, as in two dimensions, in the calculations presented here: K is taken as 0·40.

4. Two points of uncertainty

4.1. *Status of the boundary-layer approximation*

This approximation, as used above, implies the neglect of spanwise and chordwise gradients of stress and velocity in comparison with gradients normal to the surface, and clearly breaks down near wing-body junctions and wing tips as well as near separation lines, but we expect it to be valid as long as the free-stream velocity or the inner boundary condition do not change appreciably over distances of order δ. A special deduction from this approximation is that the boundary layer on a flat plate in zero pressure gradient should be unaltered by leading edge sweep as long as the co-tangent of the sweep angle is much more than $d\delta/dx$. Laminar boundary layers are certainly unaltered, but in that case the so-called 'independence' principle also holds and the motion normal to the generators on *any* infinite yawed wing is independent of that parallel to the generators: in turbulent flow the two principles cannot hold simultaneously and there has been some controversy in the past as to which, if either, is true. According to the present model equations the independence principle certainly does *not* hold because τ_z appears in the equation for τ_x (via the factor $|\boldsymbol{\tau}| = (\tau_x^2+\tau_z^2)^{\frac{1}{2}}$ if not via the vector character of G). The experiments of Ashkenas & Riddell (1955) who measured skin friction on a flat plate at various sweep angles, support this. However, Ashkenas & Riddell's values of c_f, derived from measurements of the rate of growth of momentum thickness, $d\delta_2/dx$, do depend on sweep angle, contrary to the above deduction from the boundary-layer approximation and the present model equations. Ashkenas (1958) later re-ran the experiment and found almost the same c_f at 0° and 45° sweep, although this is not explicitly stated in Ashkenas's report and the conclusion of the earlier report seems to have gained some acceptance. Figure 1 shows c_f values from the later report: it is seen that values obtained from $d\delta_2/dx$ are independent of sweep to within the likely accuracy of measurement but are about 7 % higher than Coles's (1962) formula, which could be explained by lateral convergence of the flow, due to growth of the boundary

layers on the side walls of the wind tunnel; c_f values obtained by Ashkenas (1958) from the logarithmic law agree very well with Coles's formula. Unless the logarithmic law changes with sweep in just such a manner as to camouflage a trend in c_f, we may take figure 1 as a justification of the boundary-layer approximation as stated at the beginning of this section. Some small effects of sweep on flow directions and other quantities noted by Ashkenas can probably be attributed to cross-flow originating at the rounded leading edge of the test plate.

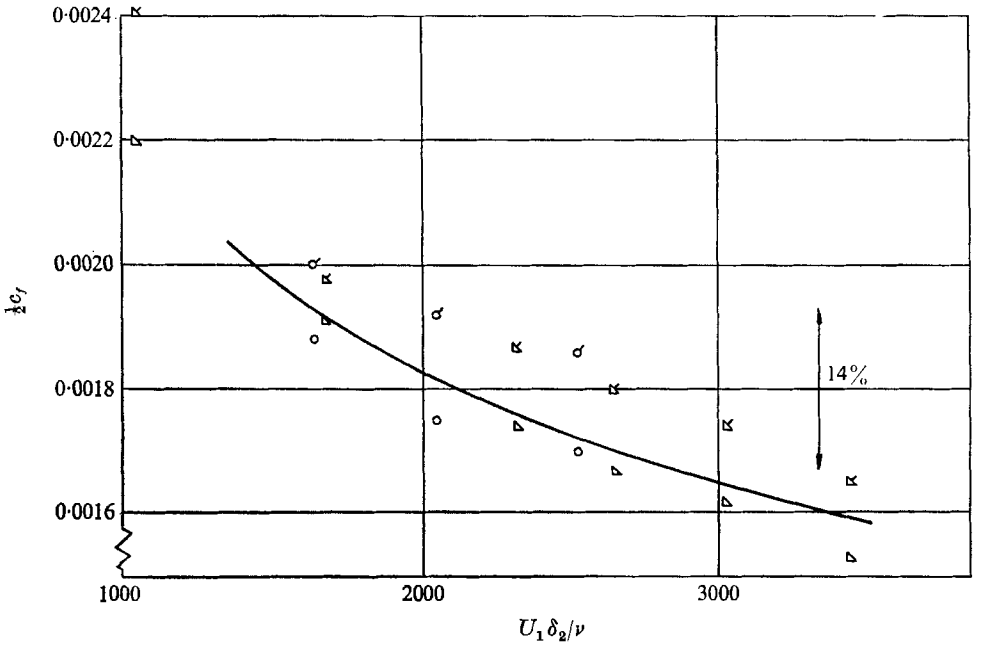

FIGURE 1. The results of Ashkenas (1958) on a flat plate. ○, no leading edge sweep; △, 45° sweep (plain symbols, c_f from logarithmic law; flagged symbols, c_f from momentum integral). ——, correlation of Coles (1962) for two-dimensional flow.

In some flows, the streamlines may converge or diverge strongly in plan view, and even if the letter of the boundary-layer approximation is not violated the results of Keffer (1965, 1967) in a wake suggest that divergence, if not convergence, may have some dynamic effect on the turbulence (the kinematic effect on the mean velocity components is easy to represent in a calculation method, whether for two-dimensional, axisymmetric or three-dimensional flow: see § 6). The only real evidence that the dynamic effect is negligible in typical boundary layers comes from the strongly divergent flow at the leading edge of a swept wing, whose properties can be predicted with reasonable accuracy by methods which ignore the effects of divergence on the turbulence structure (see Cumpsty & Head (1967*b*) and § 7 of the present paper). The measurements of Winter, Rotta & Smith (1968) on a waisted body of revolution were undertaken partly to investigate convergence and divergence effects, but the results were complicated by the presence of large longitudinal curvature and large ratios of boundary-layer thickness to cross-sectional radius of curvature.

4.2. *The effect of longitudinal mean vorticity*

Kuettner (1968), and Angell, Pack & Dickson (1968), have shown that longitudinal secondary vorticity, generated by turning a shear flow in its own plane, may lead to large quasi-steady longitudinal vortices in the Earth's atmosphere. Buoyancy effects (either stable or unstable) may be essential, in which case similar effects will not arise in engineering boundary layers unless the surface curvature is large. However, the turbulence structure *might* be appreciably affected if the shear stress vector is not exactly normal to the mean vorticity vector (that is, if the model equations (9) and (10) do not reduce to the mixing length formulae) and such an effect is not explicitly allowed for in (9) and (10). (In the original equations (1) and (2), it would appear in the pressure-strain and diffusion terms.) We may find, when more detailed explorations of the turbulence structure of three-dimensional flows are made, that the empirical functions a_1, L and G, which appear explicitly in (9) and (10), and the function a_3 which appears implicitly, are functions of the local or average angle between the shear stress and mean vorticity. At present there is no evidence: the curious behaviour of the shear stress measurements in Johnston's experiment (§ 8) could just possibly be blamed on an effect like this, but there is no indication that steady vortices formed.

5. Hyperbolic character of the equations and method of solution

In two dimensions the model equations (namely (9), (13) and (15) with the terms in $\partial/\partial z$ neglected) are hyperbolic, the number of characteristics (equal to the number of variables) being three. One characteristic is vertical and the corresponding ordinary differential equation, with derivatives along the characteristic (the y axis) only, is obtained by substituting from (15) for $\partial U/\partial x$ in (13). The other two characteristics are inclined to the x axis at angles γ given by

$$\tan\gamma = \frac{V + (a_1 G \tau_{\max}^{\frac{1}{2}} \pm (a_1^2 G^2 \tau_{\max} + 2a_1 \tau)^{\frac{1}{2}})/\rho^{\frac{1}{2}}}{U}. \tag{17}$$

As $y \to \delta$, $\tan\gamma \to V/U$, $[V + 2a_1 G(\tau_{\max}/\rho)^{\frac{1}{2}}]/U$: that is, one inclined characteristic coincides with the mean streamline; the other characteristic coincides approximately with the edge of the boundary layer. The ordinary differential equations along these characteristics are given by Bradshaw *et al.*

In three dimensions, substituting for $\partial U/\partial x$ as before gives a differential equation with derivatives in the y *and* z directions, so that the vertical characteristic line is replaced by the characteristic *surface* x = constant (in the special case of an infinite swept wing where $\partial/\partial z = 0$, the vertical characteristic line is recovered). The inclined characteristic lines, now four in number, *remain* lines along which ordinary differential equations are satisfied, in contrast to the behaviour of general hyperbolic equations in three dimensions, in which characteristic surfaces occur and in which the compatibility equations all contain derivatives in two directions: in the general case (for example, three-dimensional inviscid supersonic flow), the envelope of a set of characteristic surfaces is the characteristic conoid, the curve of contact of a given surface with the conoid

being called a bicharacteristic, but in the present case the conoids shrink to lines (which are obviously also the bicharacteristics) having all the properties of ordinary (two-dimensional) characteristics. The angles of inclination of the quasi-characteristic lines to the axes are most simply expressed by saying that the components of the velocity of propagation of a disturbance are (U, V', W) where V' takes the *four* values

$$V + (a_1 G_x \tau_{\max}^{\frac{1}{2}} \pm (a_1^2 G_x^2 \tau_{\max} + 2a_1 |\tau|)^{\frac{1}{2}})/\rho^{\frac{1}{2}},$$
$$V + (a_1 G_z \tau_{\max}^{\frac{1}{2}} \pm (a_1^2 G_z^2 \tau_{\max} + 2a_1 |\tau|)^{\frac{1}{2}})/\rho^{\frac{1}{2}}.$$

The reason for the degeneracy of the characteristics is that, in accordance with the boundary-layer approximation, we neglect turbulent transport in the x and z directions and take account of it only in the y direction. The actual rates of turbulent transport of mass, momentum or energy in the three directions are of the same order but the dimension of the boundary layer in the y direction is so much smaller than the size of the body that only gradients in this direction need be considered. Clearly this argument breaks down near streamwise corners and edges, just as the neglect of x-wise momentum transport by normal stresses breaks down near separation.

The four values of V' coincide in pairs if $G_x = G_z$: we have chosen $G_x = G_z$ throughout the boundary layer in the present calculations for want of better information, but it is fairly certain that G_x and G_z are both very small in the inner layer so that near-coincidence will occur there in any case.

This coincidence of the characteristics makes it impossible to use the 'method of characteristics' directly because that method requires as many distinct compatibility equations as there are variables. However, since the coupling between the U, τ_x and W, τ_z fields does not involve derivatives and is in any case very weak, occurring only by virtue of the presence of $|\boldsymbol{\tau}| = (\tau_x^2 + \tau_z^2)^{\frac{1}{2}}$ in both equations (9) and (10), we can use the method of characteristics separately on U, τ_x and W, τ_z, taking the other component of $|\boldsymbol{\tau}|$ as known and then, if necessary, update the value of $|\boldsymbol{\tau}|$ and iterate to improve the numerical accuracy. This technique is not very accurate near a spanwise separation line, where $\tau_z/\tau_x \to \infty$. In the case of the infinite swept wing (a swept wing of 'infinite' aspect ratio) where only one spanwise station need be calculated, the only major changes from the two-dimensional program are that the main calculation blocks for U and τ_x are repeated for W and τ_z (equality of G_x and G_z means that the blocks are almost identical). In the fully three-dimensional case, two-dimensional interpolation in the y, z plane replaces one-dimensional interpolation in the y direction and it may be that a rectangular-mesh implicit method such as that of Ferriss (1969) would be more efficient than the method of characteristics. It would certainly enable a variable y step to be used efficiently so that the first of n points could be taken at the edge of the sublayer instead of at $y = \delta/n$: this would improve the accuracy of satisfying the boundary condition, especially in rapidly changing flows. The quasi-characteristic method used for the calculations presented here seems to be adequate for all but rapidly changing flows. The cumulative numerical error in the momentum thickness is shown in figure 3 as an example of the accuracy in a very severe case.

The behaviour of the characteristics is discussed in more detail by Martin &

Ferriss (1969), principally for the case mentioned in § 2 where the $\cos\theta$ term is retained and the characteristics do not coincide in pairs unless $G_x = G_z = 0$; in this case another modification of the method of characteristics can be used for solution.

6. The present computer program

The program developed at NPL, using the above-mentioned quasi-characteristic method, is basically for the case of incompressible flow over an 'infinite' swept wing, with the isobars everywhere parallel to the generators. This is less restrictive than it sounds because (i) the infinite swept wing is an adequately general test case for the turbulence assumptions; (ii) an allowance can be made for moderate isobar convergence to extend the calculations to tapered swept wings and similar practical cases; (iii) an extension to compressible flow can be made on the lines of Bradshaw & Ferriss (1971).

The infinite swept wing is a general test case, except for the possibility of dynamic effects of streamline convergence, because no mean gradients with respect to z appear on the right-hand sides of (1) to (12): the operator D/Dt on the left-hand sides is an abbreviation for $\partial/\partial t + U\partial/\partial x + V\partial/\partial y + W\partial/\partial z$ but the character of the solution is unaltered by the relative size of the four terms. Indeed, demonstration calculations have been made for unsteady flow over an infinite plate, using the same turbulence assumptions as in steady flow (Bradshaw 1969*a*). The *numerical* problem of dealing with more than two independent variables is not trivial, and since the only suitable test data are for flows over infinite swept wings we programmed this case first. Nash (1969) has programmed his isotropic-eddy-viscosity version of the present method for fully three-dimensional flow and Wesseling (private communication) is programming the general case of flow over a surface with compound curvature.

The NPL infinite wing program, like the various two-dimensional programs, contains an allowance in the continuity equation for spanwise convergence or divergence of the flow. This was originally inserted to permit useful comparisons with nominally two-dimensional wind tunnel data, in which the flow converges in plan view because of the growth of boundary layers on the side walls, and with measurements on bodies of revolution. However, the same procedure can be used as a first approximation in three-dimensional flow, treating a given chordwise section of a tapered swept wing as an infinite swept wing with the same chordwise pressure distribution and the same spanwise convergence of the external streamlines: this is the 'axisymmetric analogy' of Eichelbrenner & Oudart (1955), although the present use of it to cope with small departures from infinite swept wing conditions is more advanced than its original application to small departures from two-dimensional flow.

Fortran listings and cards for the NPL program, together with running instructions, are available from the author at Imperial College: the running time is about half as long again as the two-dimensional method (the calculation of § 8·2 took 10 sec on a CDC 6600, which has a multiplication time of 1 μsec: the cost of central processor time was 2*s*. 3*d*.). In the general case the running time would be proportional to the number of spanwise stations.

7. Flow at the attachment line

The flow at the leading edge attachment line is in the z (spanwise) direction, τ_x and U both being zero, so that the method of characteristics will not march in the x direction. As with other methods of solution, the momentum and shear stress equations for U and τ_x must be differentiated with respect to x (measured around the surface, normal to the leading edge). For the simplest case of the infinite swept wing (with $\partial/\partial z = 0$) we easily obtain equations for $\partial U/\partial x = S$ and $\partial \tau_x/\rho\,\partial x = T$ so that the set to be solved is:

x-momentum differentiated,

$$V\frac{\partial S}{\partial y}+S^2=\frac{\partial T}{\partial y}+\left(\frac{dU_1}{dx}\right)^2; \tag{18}$$

τ_x differentiated,

$$\frac{1}{2a_1}\left(V\frac{\partial T}{\partial y}+ST\right)=\frac{\tau_z}{\rho}-\frac{(\tau_z/\rho)^{\frac{1}{2}}}{L}T-\frac{\partial}{\partial y}\left(G\left(\frac{\tau_{z_{\max}}}{\rho}\right)^{\frac{1}{2}}T\right); \tag{19}$$

z-momentum,

$$V\frac{\partial W}{\partial y}=\frac{1}{\rho}\frac{\partial \tau_z}{\partial y}; \tag{20}$$

τ_z,

$$\frac{1}{2a_1\rho}V\frac{\partial \tau_z}{\partial y}=\frac{\tau_z}{\rho}\frac{\partial W}{\partial y}-\frac{(\tau_z/\rho)^{\frac{3}{2}}}{L}-\frac{\partial}{\partial y}\left(G\left(\frac{\tau_{z_{\max}}}{\rho}\right)^{\frac{1}{2}}\frac{\tau_z}{\rho}\right); \tag{21}$$

continuity,

$$S+\partial V/\partial y=0. \tag{22}$$

These are ordinary differential equations, containing derivatives only in the y direction ($\partial U_1/\partial x$ being a known constant). Equations (20) and (21) for the flow along the leading edge depend on (18) and (19) for the flow normal to the leading edge only *via* (22): the flow along the leading edge is not the same as the quasi-radial flow on a tunnel floor with diverging sidewalls, or on a body of revolution, because $\partial U/\partial z$ is not simply $W/(z-z_0)$ where z_0 is the apparent origin of the radial flow: if we *define* a quantity z_0 by $\partial U/\partial x = W/(z-z_0)$, it is a function of y in the present case but a constant in quasi-radial flow.

We can use the logarithmic law

$$W=\frac{(\tau_{z_w}/\rho)^{\frac{1}{2}}}{K}\left[\log\frac{(\tau_{z_w}/\rho)^{\frac{1}{2}}y}{\nu}+A\right],$$

or the W-component version of (16), as the boundary condition on W and τ_z at a point just outside the viscous sublayer ($y = 0+$). τ_{z_w} is the value of τ_z at $y = 0+$. If we assume that the flow in the viscous sublayer is quasi-radial so that $U/W = \tau_x/\tau_z$, the boundary condition on S derived from the simple logarithmic law is

$$S=\frac{\rho^{\frac{1}{2}}T_w}{\tau_{z_w}^{\frac{1}{2}}K}\left[\log\frac{(\tau_{z_w}/\rho)^{\frac{1}{2}}y}{\nu}+A\right]$$

at $y = 0+$, with $T = T_w$. At the outer edge of the boundary layer $S \to dU_1/dx$, $T \to 0$, $W \to W_1$ (known) and $\tau_z \to 0$. If we make all velocities dimensionless with W_1, all shear stresses dimensionless with ρW_1^2 and all lengths dimensionless with ν/W_1 then the equations remain as written, except that $\nu = 1$ in the logarithmic

law and $(dU_1/dx)^2$ becomes $\nu^2(dU_1/dx)^2/W_1^4$ which is $1/C_*^2$ in the notation of Cumpsty & Head (1967*b*). The outer boundary conditions become $S \to 1/C_*$, $T \to 0$, $W \to 1$, $\tau_z \to 0$: the value of transformed y (equals $W_1 y/\nu$) is large at the edge of the boundary layer (varying from about 3000 to 10000 as C_* varies from 10^5 to 5×10^5). '$y = 0+$' corresponds to $(\tau_z/\rho)^{\frac{1}{2}} y/\nu \simeq 30$ or 'transformed y' $\simeq 500$ but can be taken much nearer the surface for arithmetical convenience without causing appreciable errors outside the sublayer.

8. Test cases

8.1. 45° '*infinite*' *swept wing* (*Bradshaw & Terrell* 1969)

This experiment was set up especially as a test case for the assumptions made in the outer layer: it can be regarded as a three-dimensional version of the 'relaxing' flow described by Bradshaw & Ferriss (1965) although the initial retarded flow was simply that at the trailing edge of an aerofoil-shaped fairing on the front of a flat plate, and not an equilibrium flow as in the two-dimensional case. The thickness of the fairing, and therefore the pressure gradient, was severely restricted by the 9 in. height of the tunnel, but a cross-flow angle of about 7·5° was attained at the 'trailing edge', at which the measurements started. The pressure gradient is negligible downstream of the 'trailing edge' so that the cross-flow decays, and the streamwise flow returns to constant-pressure equilibrium, solely under the action of the shear stress. Prediction of the cross-flow decay is therefore a good test of the assumptions in the calculation method: since the cross-flow is small, the agreement between calculation and experiment for the *streamwise* flow is essentially a test of the two-dimensional method (and of the experimental accuracy), but the accuracy of prediction of the cross-flow is not likely to depend on its magnitude unless the cross-flow is very large, so that the only disadvantage of small cross-flow is that measurements of cross-stream components of velocity and shear stress are difficult.

Comparisons between theory and experiment are shown in figure 2. Note that in figures 2 to 4 results are plotted against distance measured along the tunnel centre-line and not normal to the generators: with 45° sweep, the ratio is simply $\sqrt{2}$; axial distance is more meaningful for flows that begin, or end, as two-dimensional. Considering that the cross-stream shear stress is small and that what is actually measured is the component normal to the velocity vector, the agreement between calculated and measured shear stress is satisfactory, the trend of difference between the shear stress direction and the velocity gradient direction being well predicted: the detailed discrepancies are largely experimental scatter. The cross-flow angle at the surface, which is the quantity of most practical interest, is predicted very accurately. The cross-flow profiles tend to a self-preserving state.

The scatter in direction of the velocity gradient in the first few calculated profiles is a legacy of the input profile: in the computer data output, gradients are found by simple differences and the scatter on the input profile is enormous (figure 2(*c*)) although the velocity profiles are of respectable accuracy; in reducing the experimental results, smoothing was introduced.

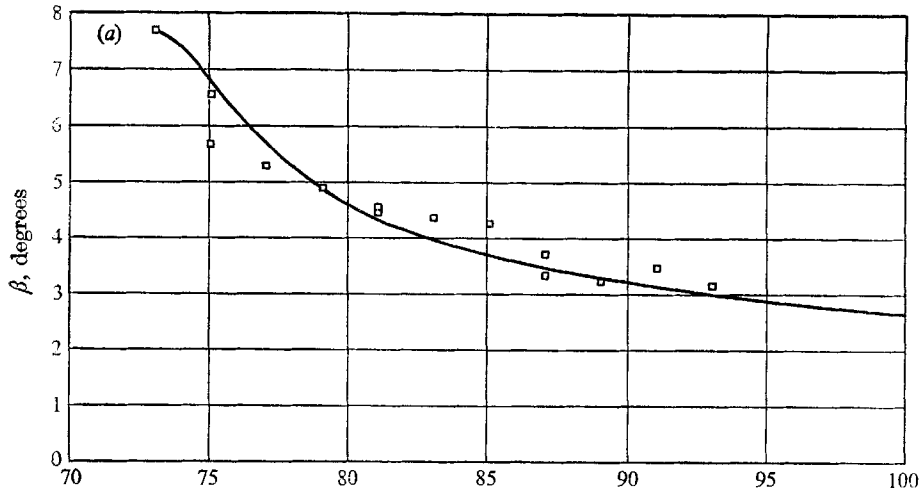

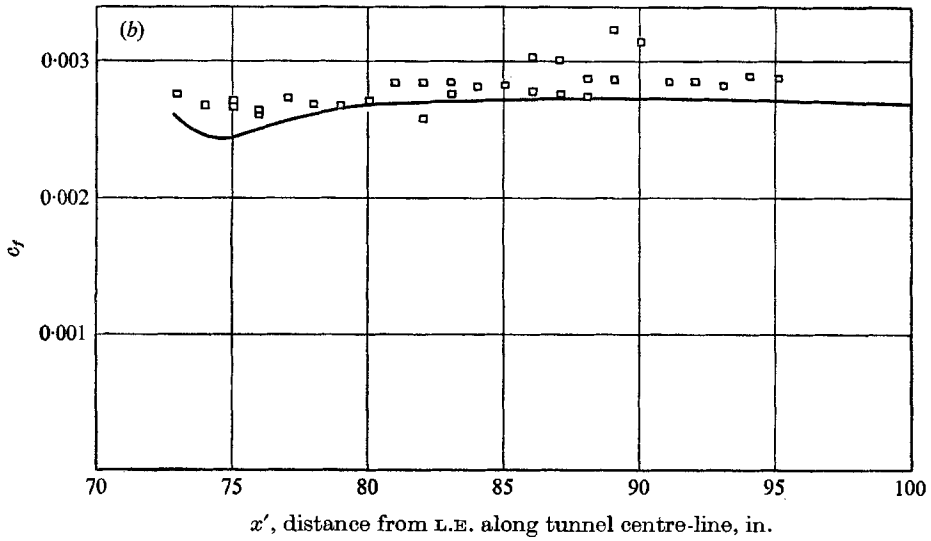

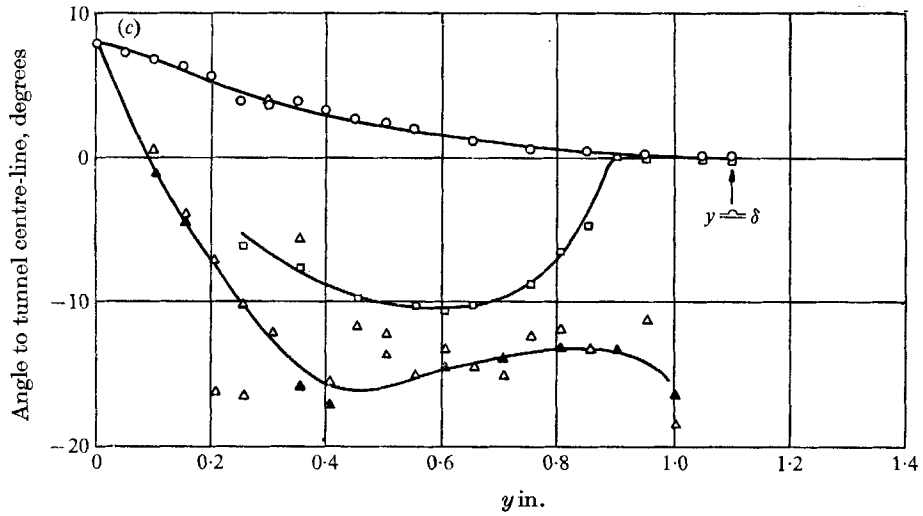

FIGURE 2. For legend see p. 433.

8.2. 45° '*infinite*' *swept plate with externally-imposed pressure gradient* (*Etheridge* 1970)

The pressure gradient, imposed by a swept cylinder above the plate, was at first strongly favourable and then moderately adverse. Values of $(\nu\rho^{\frac{1}{2}}/\tau_w^{\frac{3}{2}}).dp/dx$ approached 0·01 so that reverse transition (Patel & Head 1968; Bradshaw 1969*b*) may have been imminent. However, the predictions of surface cross-flow angle and momentum thickness shown in figure 3 are quite satisfactory (in this figure, H_{11} is the streamwise shape parameter, i.e. the ratio of the streamwise displacement thickness δ_{11} to the streamwise momentum thickness θ_{11}, and β is the surface

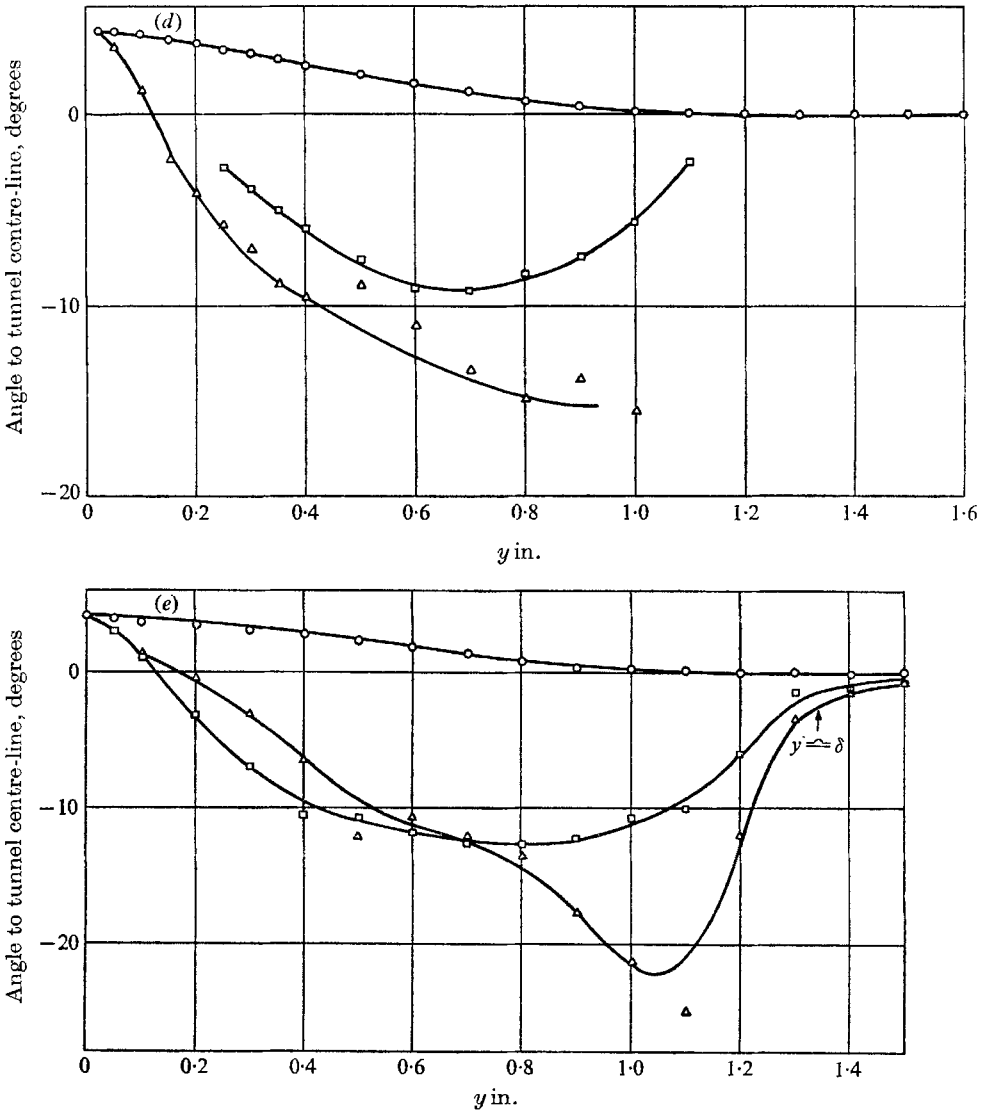

FIGURE 2. For legend see facing page.

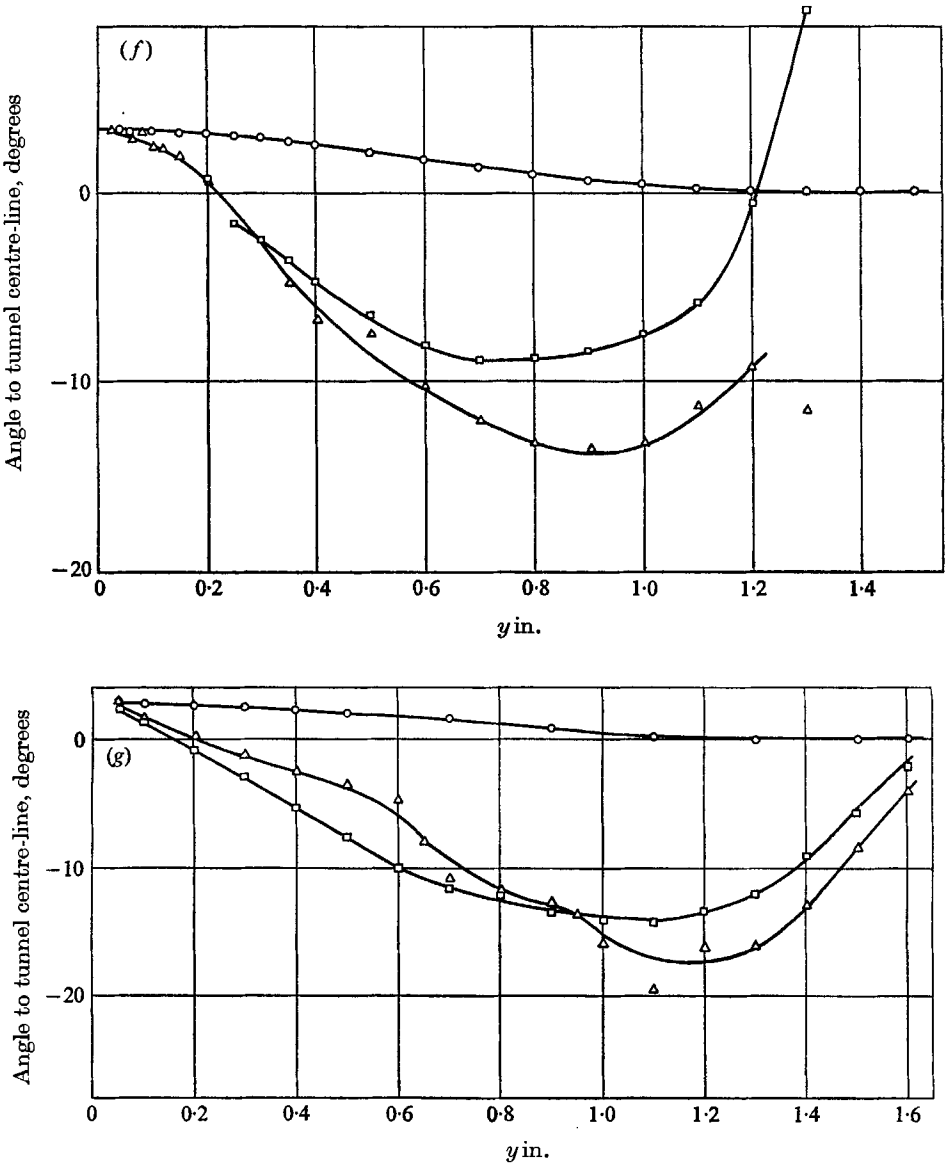

FIGURE 2. 45° 'infinite' swept wing (Bradshaw & Terrell 1969). Calculations start at $x' = 73$ in., where the boundary-layer thickness is about 1·1 in. (*a*) Surface cross-flow angle (direction of surface shear stress) with respect to tunnel axis. □, experiment, ——, calculation. (*b*) Magnitude of surface shear stress. □, experiment; ——, calculation. (*c*) Yaw angles, $x' = 73$ in. (experiment and calculation input). ○, direction of velocity; □, direction of shear stress; △, direction of velocity gradient (by simple differences); ▲, velocity gradient (smoothed). (*d*) Experimental yaw angles, $x' = 83$ in. (*e*) Calculated yaw angles, $x' = 83$ in. (*f*) Experimental yaw angles, $x' = 93$ in. (*g*) Calculated yaw angles, $x' = 93$ in.

cross-flow angle measured with respect to the local free-stream direction). Predictions of H_{11} are consistently low (even for the input profile, so that numerical errors in evaluating H_{11} from the velocity profile are at least partly to blame). These comparisons show that the present calculation method is capable of

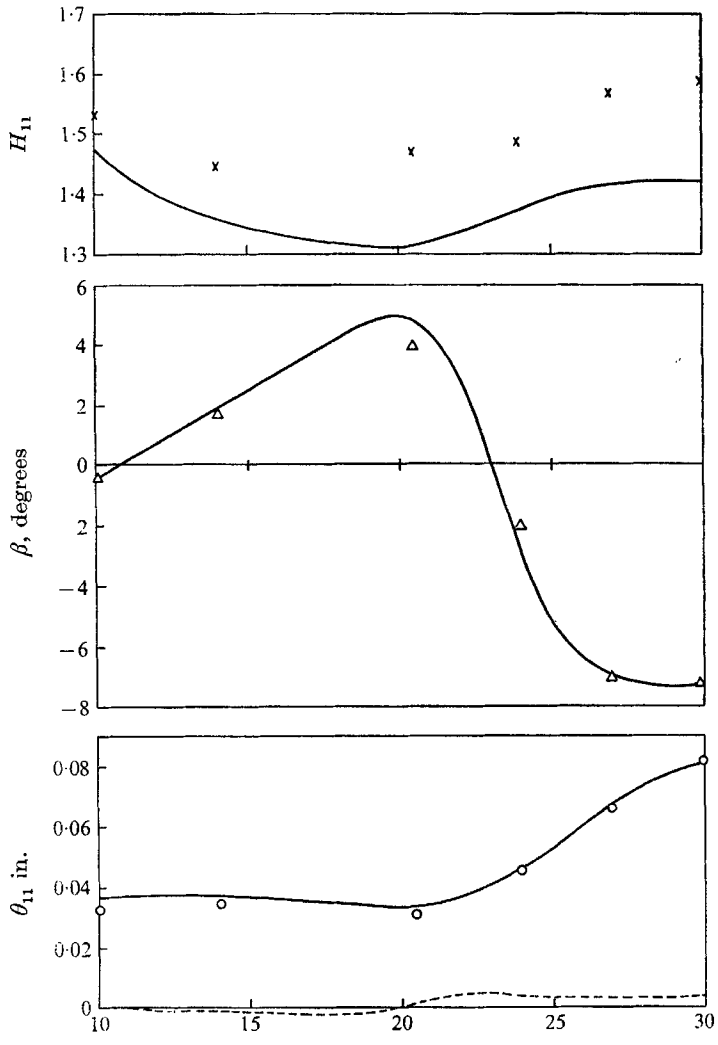

FIGURE 3. 45° 'infinite' swept wing (Etheridge 1970). Symbols: experiment. ——, calculation; – – – –, cumulative numerical error in θ_{11} deduced from the momentum integral equation.

handling rapid changes of cross-flow direction—the resulting 'cross-over' profiles, with a reversal of yaw angle with respect to the free stream, do not present any difficulties in finite difference 'field' methods although they are difficult to represent in integral methods. The rapid change in pressure gradient led to some numerical error in θ_{11} (see figure 3): errors are usually much less than this.

8.3. 45° '*infinite*' *swept forward-facing step* (*Johnston* 1970)

This experiment was set up to check the limits of accuracy of the 'mixing length' formula near the surface: the step height was 2 in., the boundary-layer thickness at $x = -17$ in., near the start of the pressure gradient, being 2·1 in. The flow in the outer part of this strongly retarded boundary layer depends far more on the pressure gradient than on the shear stress gradient. From the point of view of justification of the need for rate equations for shear stress, the most interesting result of the experiment was the appearance of large angles of lag between the shear stress and the velocity gradient in the outer layer, although such large angles will occur only in flows driven by strong pressure gradients, where, as implied above, the behaviour of the shear stress is not very important. In Johnson's experiment the pressure varied considerably in the y direction, so we cannot expect good quantitative agreement between experiment and the calculation, which was done using the *surface* pressure (in fact the prediction of c_f and surface streamline angle is quite good: as was shown by Bradshaw (1968), the hyperbolic nature of the present model of turbulence permits prediction of c_f up to separation, given the surface pressure distribution and initial conditions, despite the failure of the boundary-layer approximation, and probably the turbulence model, in the outer part of the flow). The main point of the comparisons in figure 4 is that the experiment confirms that the directions of shear stress and velocity do coincide near the surface but that the angle between the two is large in the outer part of the flow.

In the outer layer, Johnston's measured shear stress vector, figure 4 (*c*), changes direction in the opposite sense from that predicted. It is very difficult to see why the shear stress vector should rotate in the opposite direction to the velocity gradient vector: the present calculation method predicts that it should merely lag behind the velocity gradient. The discrepancies in shear stress angle are only a few degrees and may possibly be attributed to experimental error (this situation is a much more difficult one than a conventional swept wing). The eccentricities in the calculations near the wall merely show that the numerical method will not cope with such violent pressure gradients: the velocity profile extrapolates smoothly to the surface shear stress direction and both are fairly reliable, but the change in shear stress direction between the wall and the first calculation point is over-estimated. In the outer layer the velocity vector and velocity gradient vector are inclined at nearly equal and opposite angles to the undisturbed flow direction as predicted by inviscid-flow theory (values at the outer edge are nearly 0/0 and are unreliable); closer to the surface the velocity gradient vector is further rotated by the shear stress; nearer still to the surface numerical errors appear, especially at larger x.

8.4. 62·5° '*infinite*' *swept wing* (*Cumpsty & Head* 1970)

The boundary layer separated at about 80 % chord: the measured profiles were affected by traverse gear 'blockage', probably because of upstream influence of the disturbance caused to the separated flow by the wake of the traverse gear. Skin friction was not measured, so that spanwise convergence due to boundary

growth on the sidewalls cannot be estimated; the quoted sweep angle of 62·5 degrees is an 'effective' angle deduced from the isobars.

The calculations in figure 5 start from the pressure minimum: calculations by Dr B. G. J. Thompson (private communication) using a version of Cumpsty & Head's entrainment method are also shown. It will be noticed that the inclusion of a correction for the effects of surface curvature (a 'centrifugal' body force) on the turbulence makes a considerable difference to the results. To derive a three-dimensional version of the empirical correction formula suggested by Bradshaw (1969*c*) on the basis of an analogy between the effects of curvature and of

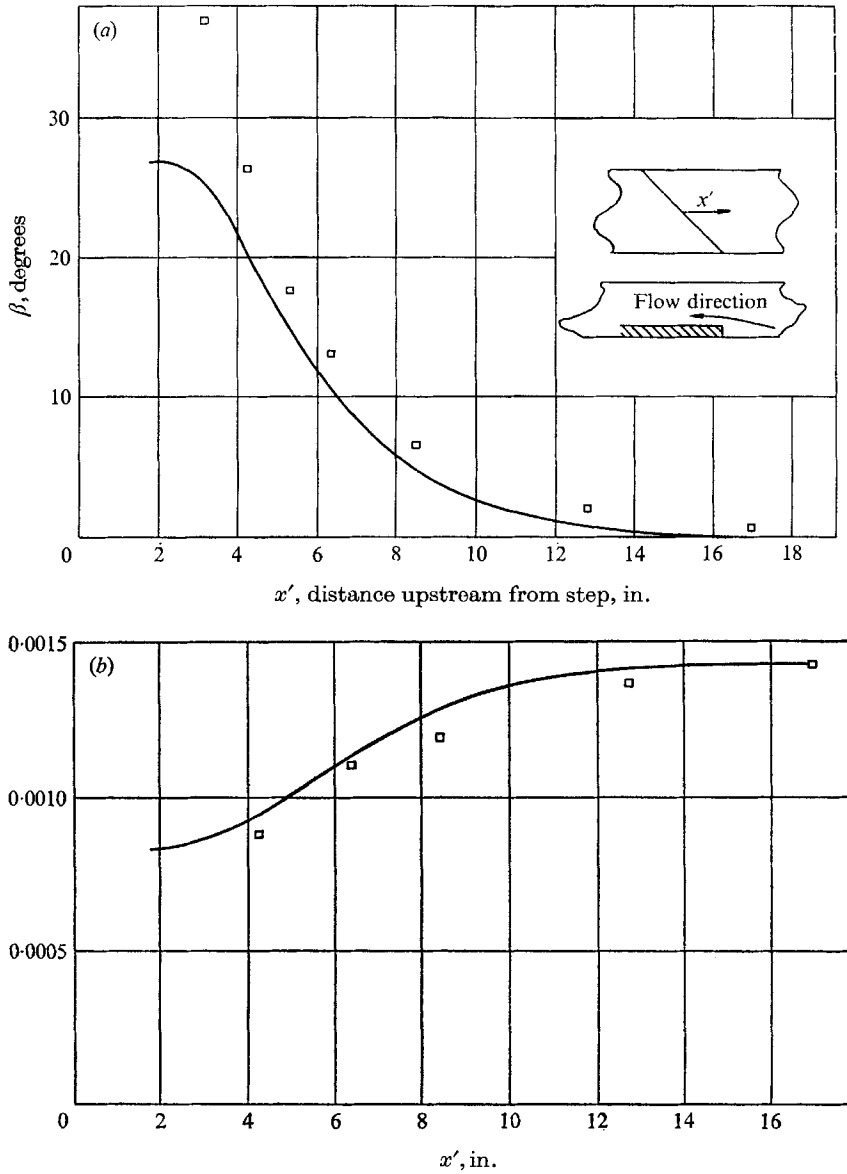

FIGURE 4. For legend see facing page.

buoyancy, we consider the 'Richardson' number in the form Ri = (Brunt–Väisälä frequency/turbulence frequency)^2. To calculate the Brunt–Väisälä frequency, ω_{BV}, we want the radius of curvature of a streamline in a plane normal to the surface, R_s, and the velocity along that streamline, U_s: then

$$\omega_{BV}^2 = 2(U_s/R_s^2)\,(\partial U_s/\partial y)\,R_s.$$

On a developable surface we can simply take U_s to be the component of velocity normal to the generators, U, and R_s to be the radius of curvature in a plane normal to the generators, R. For the turbulence frequency we take the resultant velocity gradient or, better, $|\boldsymbol{\tau}/\rho|^{\frac{1}{2}}/L$. Thus the 'Richardson' number is, to first order,

$$Ri = \frac{2(U/R)\,\partial U/\partial y}{|\boldsymbol{\tau}/\rho|/L^2} \simeq \frac{2(U/R)\,(\tau_x/\rho)^{\frac{1}{2}}/L}{|\boldsymbol{\tau}/\rho|/L^2} = 2\frac{U}{R}\frac{(\tau_x/\rho)^{\frac{1}{2}}}{|\boldsymbol{\tau}/\rho|}L.$$

As in two dimensions we use the 'Richardson' number to divide L by the factor $1 + 7Ri$ (on a convex surface) derived from meteorological data. The effects of the curvature correction in figure 5 are large enough to cast doubt on the accuracy of the first-order formula used here—which is itself rather speculative—so that the final conclusion is that the predictions of the calculation method are, at worst, not incompatible with Cumpsty & Head's results, particularly the separation position, which was measured in the absence of the traverse gear. Thompson's calculation does not contain any curvature correction and would presumably change as much as the present calculation if a correction were inserted: its agreement with the present calculation with curvature correction is fortuitous.

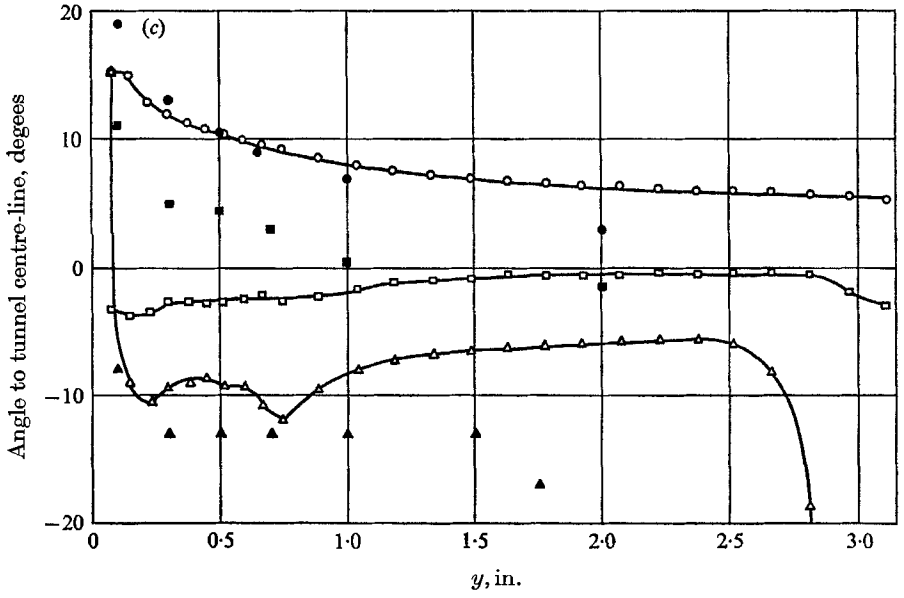

FIGURE 4. 45° ' infinite ' forward-facing step (Johnston 1970). (*a*) Surface cross-flow angle (with respect to tunnel axis). □, experiment; ——, calculation. (*b*) Magnitude of surface shear stress (U_{ref} is velocity far upstream). □, experiment; ——, calculation. (*c*) Yaw angles 4·1 in. upstream of step. Solid symbols, experiment; open symbols, calculation. ○, direction of velocity; □, direction of shear stress; △, direction of velocity gradient.

8.5. *Demonstration test cases of Cumpsty & Head* (1967*a*)

These are Cumpsty & Head's *calculations*, with a constant linear gradient of chordwise velocity ('$k = 0{\cdot}25$') and varying sweep angles. The object of the comparison is to show that, as in § 8.4, the present calculation method disagrees fairly strongly with the 'entrainment' method. Part of the disagreement on separation position (figure 6(*a*)) may be due to the crudity of the present numerical method, but the monotonic trend of the present results is more plausible than that shown by the 'entrainment' calculations, and figure 6(*c*)

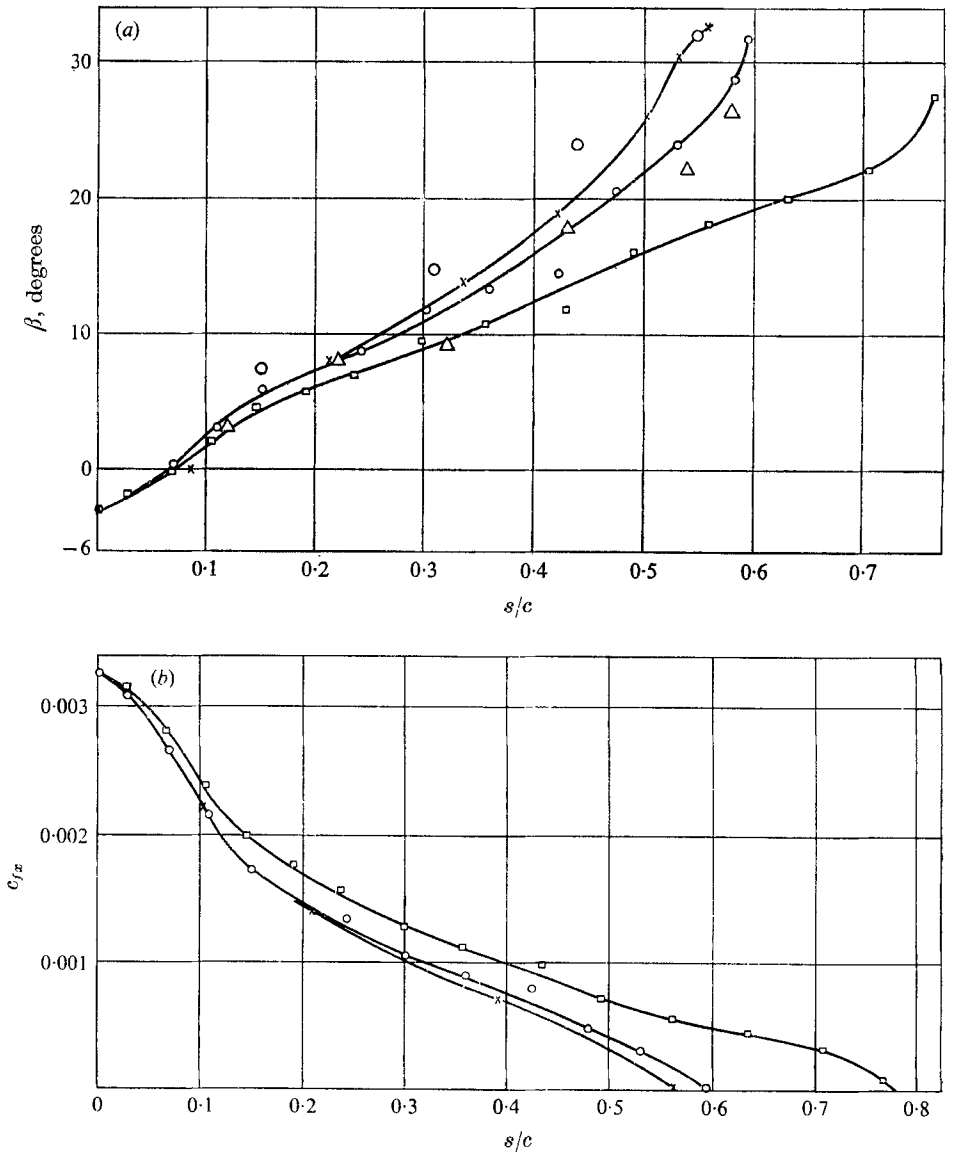

FIGURE 5. For legend see facing page.

shows that the two sets of predictions differ considerably even near the start of the calculation, especially for the larger sweep angles. Dr J. F. Nash has informed me that his version of the present calculation method, using a more refined numerical scheme but assuming that the direction of the shear stress coincides with that of the velocity gradient, shows a monotonic trend similar to that in figure 6(*a*).

A plausible explanation for the increasing disagreement between the entrainment method and the present method for large cross-flows is that Cumpsty & Head assume the entrainment to depend solely on the profile of the velocity component in the local free stream direction. Now it was shown by Bradshaw *et al.* (1967) that in two-dimensional flow the entrainment velocity correlates quite well on $\tau_{\max}/U_1$, and according to the general argument that the scalar properties of the turbulence will be unaltered by moderate three-dimensionality the entrainment in three dimensions should be roughly $10\,|\tau_{\max}/\rho U_1|$: an analogous result would follow from Horton's (1969) correlation based on τ at $y = 0{\cdot}5\delta$. Supposing that the entrainment relation used by Cumpsty & Head is exactly correct in two dimensions, it will be an underestimate in three dimensions because $\tau_{\max}$ is necessarily larger than the component of $\tau_{\max}$ in the local free-stream direction by an amount that increases with cross-flow (this argument is of course rather loose).

The streamwise shape parameter (figure 6(*d*)) has much lower values at

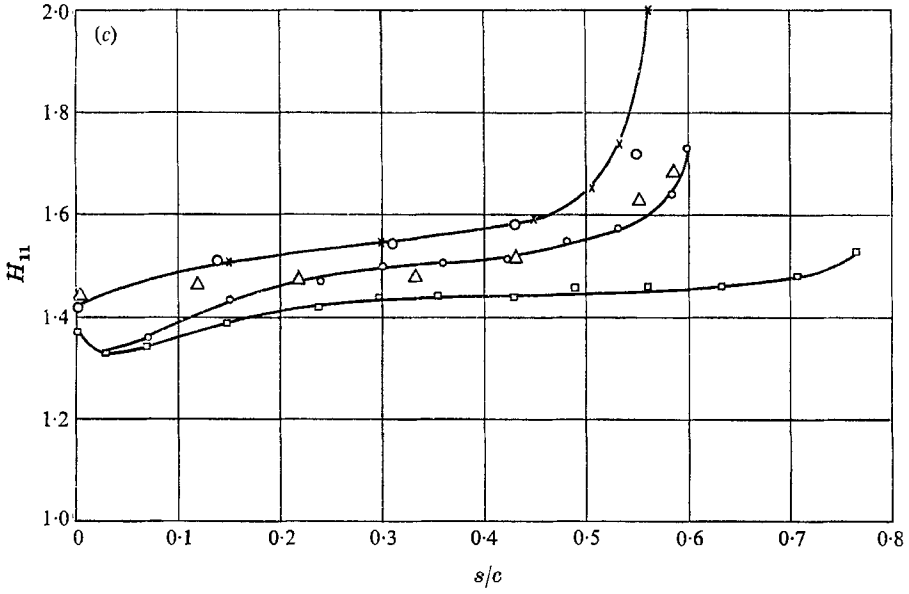

FIGURE 5. 62·5° 'infinite' swept wing (Cumpsty & Head 1969). s/c is distance normal to leading edge (origin near pressure minimum). ○, experiment with slender traverse gear; △, experiment with earlier traverse gear; □, calculation without curvature correction; ○, calculation with curvature correction, ×, calculation by entrainment method (Thompson). (*a*) Surface cross-flow angle β (with respect to local free-stream direction). (*b*) Chordwise component of surface shear stress (no experimental data: separation at $s/c = 0{\cdot}66$). (*c*) Streamwise shape parameter.

separation than in two-dimensional flow, the effect being even larger in the present calculations than in those of Cumpsty & Head. There is no real significance in this parameter when there is such a large angle between the local free stream and the flow near the wall: the shape parameter based on the velocity component normal to the generators takes values of 3 or more at separation.

The variation of crossflow angle with sweep angle (figure 6(*b*)) is odd at first sight, but becomes plausible when one remembers that at sweep angles near 90°

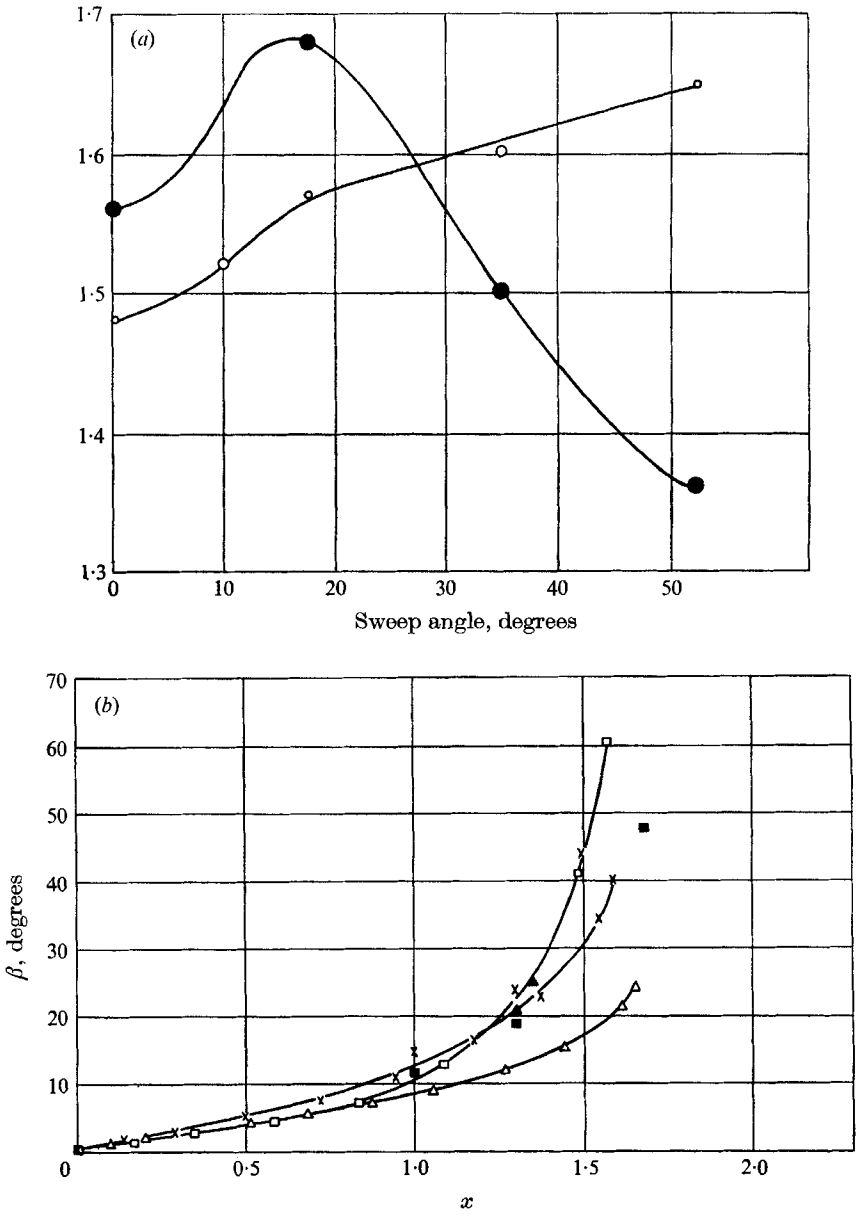

FIGURE 6. For legend see facing page.

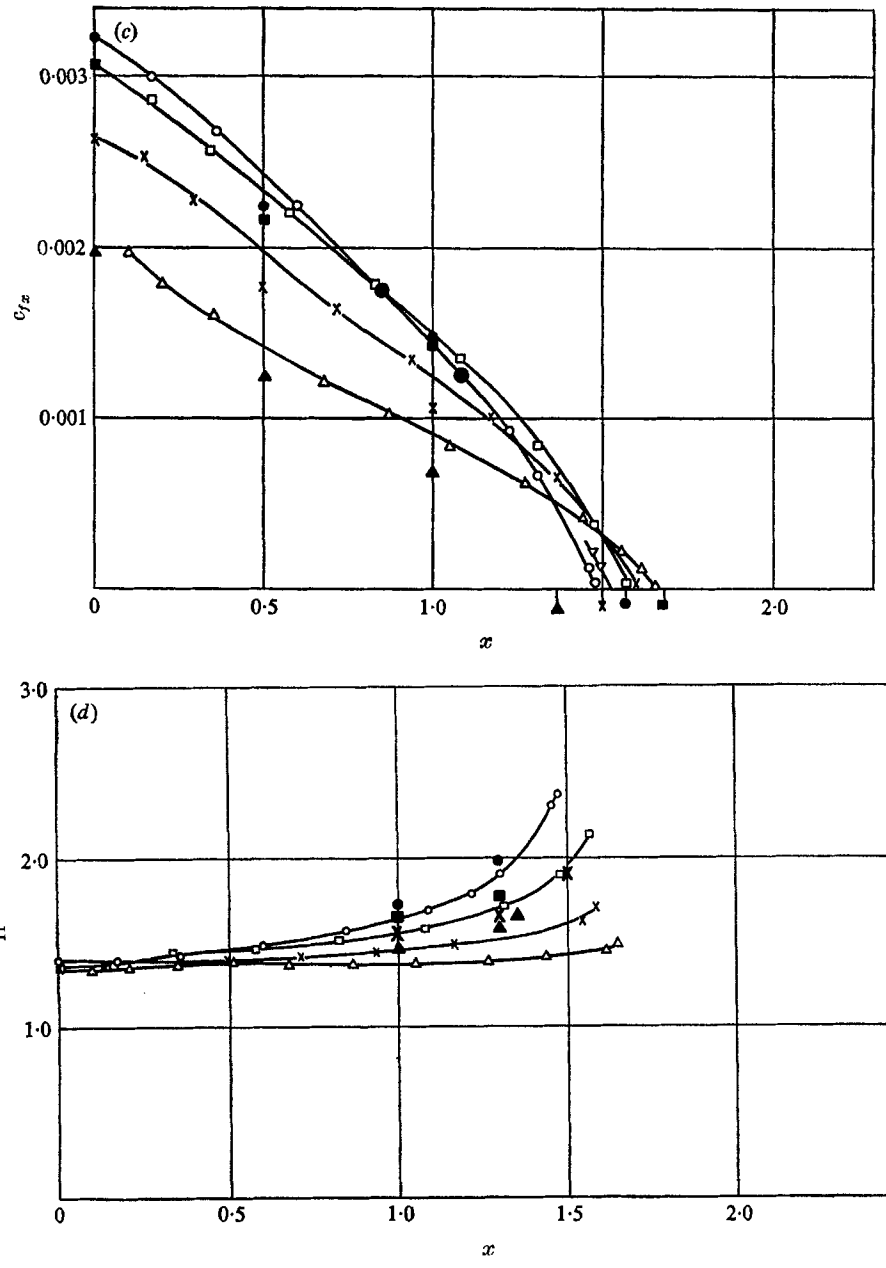

FIGURE 6. 'Infinite' swept wing demonstration calculations of Cumpsty & Head (1967*a*) '$k = 0{\cdot}25$'. x is dimensionless distance measured normal to leading edge. Solid symbols, Cumpsty–Head calculations (entrainment method); open symbols, present calculations. (*a*) Separation position at different sweep angles. (*b*) Surface cross-flow angle β (with respect to local free-stream direction). □, 17·5° sweep; ×, 35°; △, 52·4°. Last symbol is at separation point in each case. (*c*) Chordwise component of surface shear stress. ○, zero sweep; ▽, 1° (near separation only); □, 17·5°; ×, 35°; △, 52·5°. (*d*) Streamwise shape parameter (for symbols see figure 6(*c*)).

the cross-flow is always small, even at separation, and that at very small sweep angles the cross-flow angle is small except very near separation, where it rises to nearly 90°. In the limiting case of two-dimensional flow the cross-flow angle at separation is indeterminate (0/0): in practical cases it *will* rise to 90° because of manufacturing imperfections or non-uniformity of the tunnel stream direction. Although the cross-flow angle is the simplest measure of three-dimensional effects it depends on the ratio of the components of surface shear stress normal and parallel to the local free stream, and we saw in § 2 that perpendicular components of shear stress are quite loosely coupled so that large variations in their ratio have no great physical significance.

8.6. *Attachment line flow*

The ordinary differential equations (18)–(22) have been solved for a sample case, $C^* = 3 \times 10^5$. There are no cross-flow measurements for comparison, but the results (figure 7) are included here for use in starting calculations by the main method at a point just behind the leading edge. For simplicity, we used Runge–Kutta integration starting from guessed values of T and τ_z, implying values of S and W from the logarithmic law, at $y = 0+$ (actually about $0{\cdot}03\delta$). The initial values, and the boundary-layer thickness chosen to scale L and G, were adjusted by trial and error until the outer boundary conditions were satisfied: the behaviour near the outer edge of W and S, particularly the latter, was very sensitive to the choices of T_W and τ_{z_w}, which meant that T_w and τ_{z_w} could soon be found quite accurately. The results confirm the finding of Cumpsty & Head that τ_z/W_1^2 is a little lower than in a two-dimensional boundary layer in zero pressure gradient at the same momentum-thickness Reynolds number. The T profile looks like the shear stress profile in a highly-accelerated two-dimensional boundary layer. The rate of increase of wall streamline angle with x is about 1·3 times the rate of increase of external streamline angle. The quantitative results at this low Reynolds number (about 500 based on momentum thickness) are not as accurate as at higher Reynolds numbers because the method does not take account of viscous effects on the outer layer (Coles 1962, appendix A): further work on this is in progress. Cumpsty & Head's calculations, based on an empirical entrainment relation, agree rather better with their measurements of the velocity component along the leading edge than do the present calculations. The differences between the calculated and experimental W profiles (figure 7) are rather too large to be due to any likely error in calculating the cross-flow (for which no experimental profiles are available): the remaining possibilities are numerical or experimental error or the effect of low Reynolds numbers: the long 'tail' on the experimental profile (small wake component—see Coles 1962) suggests the last-named cause, although as mentioned above the outer part of the calculated profile is rather uncertain.

9. Conclusions

The two-dimensional calculation method of Bradshaw *et al.* (1967), based on an empirical shear stress equation, has been extended to three dimensions (two components of shear stress) without using more empirical data (strictly, data

are needed to establish the vector character of the diffusion term but the present quasi-scalar approximation should serve for engineering calculations). Such extensions of the basic method seem to be relatively straightforward (Bradshaw 1970), because of the close relation between the empirical shear stress equation

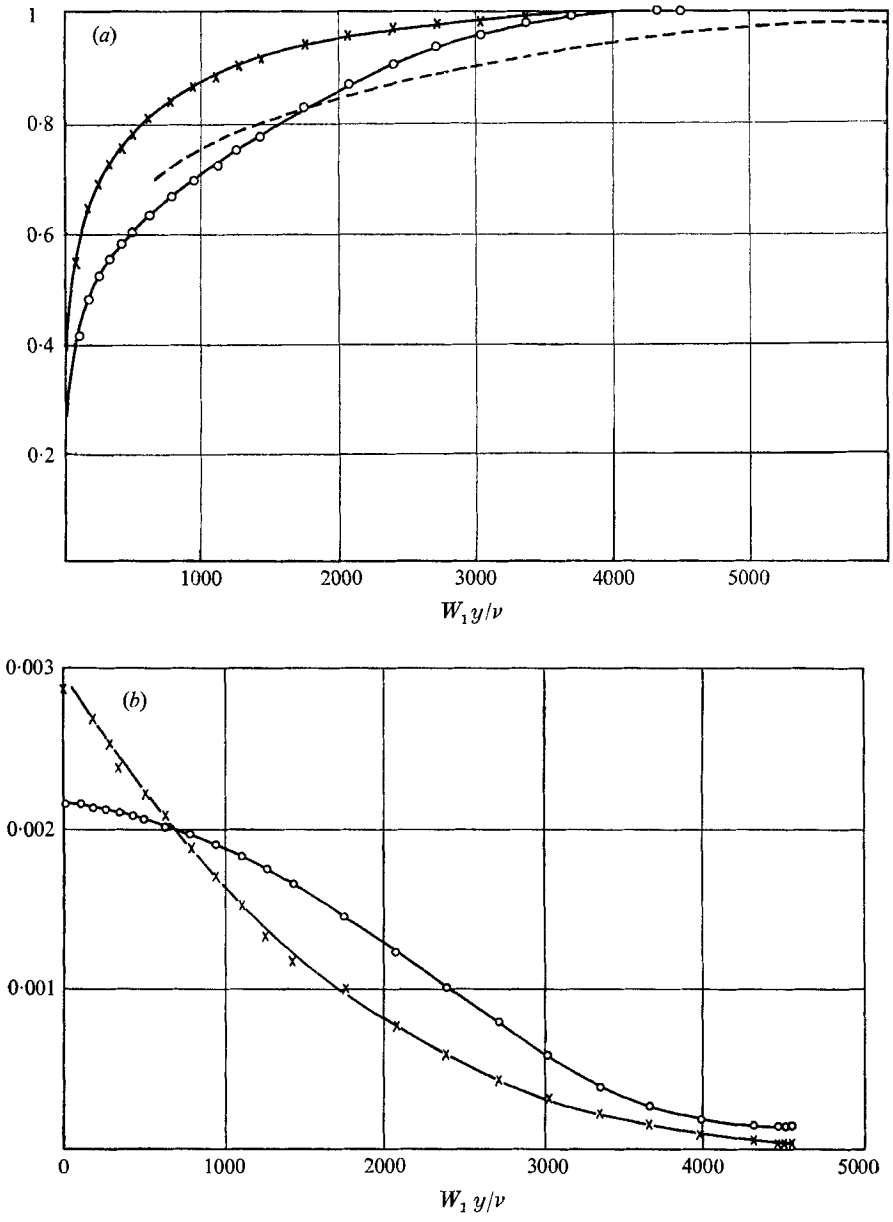

FIGURE 7. Attachment-line boundary layer (z axis along leading edge)

$$C^* = W_1^2/(\nu\, dU_1/dx) = 3 \times 10^5.$$

(a) Velocity profile components. – – –, W/W_1 (experimental; Cumpsty & Head 1969); ○, W/W_1 (calculated); ×, $(\partial U/\partial x)/(\partial U_1/\partial x)$ (calculated). (b) Calculated shear-stress profile components. ○, $\tau_z/\rho W_1^2$; ×, $(\partial \tau_x/\partial x)/(\rho W_1^2 \partial U_1/\partial x)$.

and the exact (but insoluble) shear stress equation derived from the Navier–Stokes equations. The shear-stress equations reduce to the mixing length formula (direction of shear stress equals direction of velocity gradient) when transport and diffusion terms are small: since this is expected to be the case near the surface the mixing length formula is justified here, and inner law profiles deduced from it can be used for the inner boundary condition, as in two-dimensional flow, with some reservations about its behaviour in especially strong pressure gradients. Agreement with experiment in the available test cases for infinite swept wings (an adequately general case as far as the turbulence is concerned) is within the likely uncertainties of the data and of the present computer program, which is expected to show some inaccuracy very close to separation. The extension to the fully three-dimensional and/or compressible case is solely a numerical problem: no extra data are needed and no deterioration in the accuracy is expected. The method is intended only for flows to which the boundary-layer approximation applies—that is, where streamwise and spanwise velocity gradients are small compared to those normal to the surface: flows along corners and edges are specifically excluded.

I am grateful to Dr S. C. Crow, Prof. J. P. Johnston and Dr D. W. Martin for helpful discussions on three-dimensional flows. I am indebted to Mr J. Laws for running the computer and to him and to Mr D. H. Ferriss for advice on programming. Mr Ferriss also programmed and ran the attachment-line calculations.

REFERENCES

ANGELL, J. K., PACK, D. H. & DICKSON, C. R. 1968 *J. Atmos. Sci.* **25**, 707.

ASHKENAS, H. 1958 *N.A.C.A. Tech. Note* no. 4140.

ASHKENAS, H. & RIDDELL, F. R. 1955 *N.A.C.A. Tech. Note* no. 3383.

BRADSHAW, P. 1967 *J. Fluid Mech.* **30**, 241.

BRADSHAW, P. 1968 *Nat. Phys. Lab. Aero. Rep.* no. 1232.

BRADSHAW, P. 1969*a* *Nat. Phys. Lab. Aero. Rep.* no. 1288.

BRADSHAW, P. 1969*b* *J. Fluid Mech.* **35**, 387.

BRADSHAW, P. 1969*c* *J. Fluid Mech.* **36**, 177.

BRADSHAW, P. 1970 *Imperial College Aero. Rep.* no. 70–06.

BRADSHAW, P. & FERRISS, D. H. 1965 *Nat. Phys. Lab. Aero. Rep.* no. 1145 (and Addendum 1968).

BRADSHAW, P. & FERRISS, D. H. 1971 *J. Fluid Mech.* **46**, 83.

BRADSHAW, P., FERRISS, D. H. & ATWELL, N. P. 1967 *J. Fluid Mech.* **28**, 593.

BRADSHAW, P. & TERRELL, M. G. 1969 *Nat. Phys. Lab. Aero. Rep.* no. 1305.

COLES, D. E. 1962 *Rand Corp. Rep.* no. R-403-PR and *Aero. Res. Counc. paper* no. 24497 (1963).

CROW, S. C. 1968 *J. Fluid Mech.* **33**, 1.

CUMPSTY, N. A. & HEAD, M. R. 1967*a* *Aero. Quart.* **18**, 55.

CUMPSTY, N. A. & HEAD, M. R. 1967*b* *Aero. Quart.* **18**, 150.

CUMPSTY, N. A. & HEAD, M. R. 1970 *Aero. Quart.* **21**, 121.

DONALDSON, C. DUP., SULLIVAN, R. & ROSENBAUM, H. 1970 *A.I.A.A. paper* no. 70–55.

EICHELBRENNER, E. A. & OUDART, A. 1955 *O.N.E.R.A., Paris*, pub. no. 76.

ETHERIDGE, D. 1970 Ph.D. Thesis, Queen Mary Coll., London University.

FERRISS, D. H. 1969 *Nat. Phys. Lab. Aero. Rep.* no. 1295.

HORTON, H. P. 1969 *Hawker Siddeley Aviation (Hatfield) Research Rep.* 1094/HPH.

JOHNSTON, J. P. 1970 *J. Fluid Mech.* **42**, 823.

KEFFER, J. H. 1965 *J. Fluid Mech.* **22**, 135.

KEFFER, J. H. 1967 *J. Fluid Mech.* **28**, 183.

KLINE, S. J., MORKOVIN, M. V., SOVRAN, G. & COCKRELL, D. J. 1969 *Proceedings, Computation of Turbulent Boundary Layers*—1968 *AFOSR—IFP—Stanford Conference*, Thermosciences Divn., Stanford University.

KOVASZNAY, L. S. G. & HALL, M. G. 1967 *A.I.A.A. J.* **5**, 2065.

KUETTNER, J. P. 1968 *Aero. Revue*, p. 52 and p. 109.

MARTIN, D. W. & FERRISS, D. H. 1969 *Nat. Phys. Lab. Maths. Rep.* no. 74.

NASH, J. F. 1969 *J. Fluid Mech.* **37**, 625.

PATEL, V. C. & HEAD, M. R. 1968 *J. Fluid Mech.* **34**, 371.

TOWNSEND, A. A. 1956 *The Structure of Turbulent Shear Flow.* Cambridge University Press.

WESSELING, P. 1969 *N.L.R. (Amsterdam) Rep.* no. AT-69-01.

WINTER, K. G., ROTTA, J. C. & SMITH, K. G. 1968 *R.A.E. Tech. Rep.* no. 68215.